A98-31601 ICAS-98-4,7,2

STRUCTURAL OPTIMIZATION WITH STATIC CONSTRAINTS USING EXPANDABLE MODAL BASIS

M. Karpel*and B. Moulin†
Faculty of Aerospace Engineering
Technion - Israel Institute of Technology, Haifa, Israel 32000

Abstract

The modal-based approach to aeroelastic optimization with static aeroelastic and stress constraints is extended by adding static deflection modes to the modal basis. The optimization process starts with a reduced-size model that uses low-frequency normal modes of the baseline structure as fixed generalized coordinated. Static deformations in design cases calculated along the optimization path contain local modal-perturbation information that is not included in the modal basis. These modes are orthogonalized with respect to the modal basis and added as new generalized coordinates. With this expansion, the modal-based optimization becomes more efficient and it convergences to the exact optimal design. Numerical example with realistic fighter-aircraft model demonstrates practical applications with CPU speed-up factors of 5-10, compared to the regular discrete-coordinate approach, with negligible loss of accuracy.

Introduction

The desire for efficient procedures for optimal design of complex structures motivated the development of reduced-size optimization schemes where calculations of stability and response parameters, and their sensitivity to changes in the design variables, are based on a set of low-frequency vibration modes of a baseline structure. The modal approach is especially attractive in multidisciplinary cases where the excitation loads are affected by the structural response, such as in aeroelastic and control augmented systems.

Commonly used structural analysis and optimization schemes[1-4] use the modal approach in the dynamic response and stability disciplines, but the static aeroelastic and stress disciplines are treated by the discrete approach with typically large stiffness matrices with thousands degrees of freedom. An example for a discrete-approach optimization code is the Automated Structural Optimization System (ASTROS)[1] that was developed to provide a multidisciplinary analysis and design capability for aerospace structures. The various disciplines in ASTROS include static and dynamic structural analysis, aeroelastic analysis and some features of the interaction with the control system.

The extension of the modal approach for application in optimization with static aeroelastic constraints was first presented in Ref. 5 and later integrated in an aeroservoelastic optimization scheme[6]. The modal approach was extended to deal with static stress constraints[7] by using a modal-perturbation scheme. A way to deal with local stresses due to concentrated loads by using fictitious masses was pointed out in Refs. 8 and 9. Further developments of the modal approach for problems with static aeroelastic and stress constraints, and their implementations in ASTROS, was done in Refs. 10 and 11. The ASTROS implementations take advantage of the fact that both modal and discrete structural coefficient matrices of the baseline structure are saved in the same data base and can be combined effectively throughout the optimization process. A further enhancement of the modal-based approach to optimization with static disciplines was it application with parts of the structure subjected to static condensation[12].

The formulations in Refs. 7, 10-12 used a fixed generalized coordinate basis (the normal modes of the baseline structure) throughout the optimization, with the displacement vector for stress analysis of each design case re-evaluated in every design iteration. Being affected by the modal perturbations mentioned above, these displacement vectors contain valuable information which is not contained in the normal modes. This information is used in this paper for expanding the modal basis in subsequent iterations. The use of static displacement modes as reduced-basis generalized coordinates for reanalysis was suggested in Refs. 13 and 14 with applications to truss structures under fixed loads.

Modal Equilibrium Equations

Structural analysis and optimization with aeroelastic considerations using finite-element codes such as ASTROS[1] and MSC/NASTRAN[2] start with the

*Associate Professor, Senior Member AIAA
†Research Associate

21st ICAS Congress
13-18 September 1998
Melbourne, Australia

definition of a structural model and n_{dv} global design variables. A description of the discrete coordinate sets and the associated structural matrices at the various model-construction and analysis stages is given in Appendix A. The matrices are first assembled with respect to the g-set displacement set. The application of displacement constraints reduces the model to the f-set coordinates by eliminating the dependent ones. The optional Guyan's static-condensation process omits the user-defined o-set coordinates, which reduces the model to the a-set coordinates. The partitioning out of rigid-body reference coordinates, when the structure is free, reduces the a-set model to the l-set discrete coordinates in which the equilibrium equations are solved.

The modal coordinates are based on an eigensolution with the a-set matrices $[K_{aa}]$ and $[M_{aa}]$ of the baseline structure. The resulting set of normal modes $[\phi_a]$ satisfy the eigenvalue problem

$$[K_{aa}][\phi_a] = [M_{aa}][\phi_a][\lambda] \qquad (1)$$

where $[\lambda]$ is a diagonal matrix of the corresponding eigenvalues, where the first n_r rigid-body eigenvectors are zero.

The basic assumption of the modal approach in structural analysis and optimization is that the displacements $\{u_a\}$ (static or dynamic) of the modified structure in response to external excitation can be adequately expressed as a linear combination of the baseline modes:

$$\{u_a\} = [\bar{\phi}_{ar}]\{\xi_r\} + [\phi_{ae}]\{\xi_e\} \qquad (2)$$

where $\{\xi_r\}$ and $\{\xi_e\}$ are vectors of the generalized rigid and elastic displacements, $[\phi_{ae}]$ is the matrix of n_e low-frequency elastic modes taken into account, and $[\bar{\phi}_{ar}]$ is the matrix of n_r rigid-body modes defined by enforcing $[\bar{\phi}_{rr}] = [I]$, where $[\bar{\phi}_{rr}]$ is a partition of $[\bar{\phi}_{ar}]$ associated with the rigid-body reference displacements $\{u_r\}$.

The substitution of Eq. (2) in Eq. (A-7) of Appendix A, and premultiplication by $[\phi_a]^T$ yields the equation of motion in modal coordinates, where the number of degrees of freedom, $n_r + n_e$, is typically several orders of magnitude smaller than the number of discrete degrees of freedom. In modal-based static analysis, the elastic accelerations are neglected and the modal equation becomes[10]

$$\begin{bmatrix} 0 \\ K_{ee} \end{bmatrix}\{\xi_e\} + \begin{bmatrix} M_{rr} \\ M_{er} \end{bmatrix}\{\ddot{\xi}_r\} = \begin{bmatrix} \bar{\phi}_{ar}^T \\ \phi_{ae}^T \end{bmatrix}\{P_a\} \quad (3)$$

where $[K_{ee}]$, $[M_{rr}]$ and $[M_{er}]$ are partitions of the generalized stiffness and mass matrices. $[K_{ee}]$ is diagonal and $[M_{er}] = 0$ for the baseline structure but not for the modified one. The unit contribution of each global design variable to the generalized matrices is stored in a modal data base and used to update the matrices of Eq. (3) throughout the optimization process[10]. This eliminates the need to reconstruct the discrete-coordinate matrices. Equation (3) can be solved for $\{\xi_e\}$ and $\{\ddot{\xi}_r\}$. Equation (2) can then be used to recover $\{u_a\}$ for stress/strain analysis. In static aeroelastic cases, $\{P_a\}$ is an aerodynamic loads vector which is a function of $\{\xi_e\}$ and the aircraft trim variables.

Linear static aeroelastic codes are commonly based on aerodynamic panel methods that produce Mach dependent force coefficient matrices that relate aerodynamic loads on the panels to local angles of attack. Pre and post multiplications of the panel matrices by modal deflections and slopes, transformed to the aerodynamic grid by spline techniques, generate the steady aerodynamic force coefficient matrices $[A_{rr}]$, $[A_{re}]$, $[A_{er}]$ and $[A_{ee}]$ associated with the rigid-body and elastic modal displacements. The splined modes can also be used to generate the generalized force coefficient matrices $[A_{r\delta}]$ and $[A_{e\delta}]$ where the subscript δ relates to the vector $\{\delta\}$ of trim variables such as angle of attack, control surface deflection and roll rate.

The formulation and solution of static-aeroelastic equilibrium equations in modal coordinates were presented in Refs. 10 and 11, which assumed that the static-condensation option is not used, namely $[K_{aa}] \equiv [K_{ff}]$ and $[M_{aa}] \equiv [M_{ff}]$. The effects of static condensation are formulated in Ref. 12. A general form of the equilibrium equation is

$$\begin{bmatrix} -qA_{rr} & -qA_{re} & M_{rr} \\ -qA_{er} & K_{ee} - qA_{ee} & M_{er} \\ M_{rr} & M_{er}^T & 0 \end{bmatrix} \begin{Bmatrix} \xi_r \\ \xi_e \\ \ddot{\xi}_r \end{Bmatrix} = \begin{bmatrix} qA_{r\delta} \\ qA_{e\delta} \\ 0 \end{bmatrix}\{\delta\} \qquad (4)$$

where q is the dynamic pressure. The last row in Eq. (4) relates rigid-body displacements to the elastic ones. For the baseline structure $[M_{er}] = 0$ and hence $\{\xi_r\} = 0$. However, when the structure changes, a non-zero $\{\xi_r\}$ is needed to enforce orthogonality between the elastic deformations and the rigid-body modes[10]. The elimination of $\{\xi_r\}$ and $\{\xi_e\}$ from Eq. (4) yields the trim equation

$$[M_{rr}]\{\ddot{\xi}_r\} = q[\tilde{A}_{r\delta}]\{\delta\} \qquad (5)$$

The flex-to-rigid ratios between terms in $[\tilde{A}_{r\delta}]$ of Eq. (4) and $[A_{r\delta}]$ of Eq. (5) define the aeroelastic effectiveness parameters which can be used as optimization constraints. The solution of Eq. (5) for the n_r free trim variables (where n_r is the number of rigid-body modes) and the recovery of $\{\xi_r\}$ and $\{\xi_e\}$ by Eq. (4) facilitates the calculation of the net

loads

$$\{P_a\} = [P_1]\{\delta\}+[P_2]\{\xi_r\}+[P_3]\{\xi_e\}-[M_{aa}][\phi_{ar}]\{\ddot{\xi}_r\} \quad (6)$$

where $[P_1]$, $[P_2]$ and $[P_3]$ are the aerodynamic load matrices due to the trim parameters and modal displacements.

It can be observed that the trim variables, net loads and effectiveness constraints are functions of the design variables. The differentiation of Eqs. (4-6) with respect to the design variables results in analytical sensitivity expressions[10]. The order of Eq. (4) is typically 2 to 3 orders of magnitude smaller then the equivalent one in common discrete-coordinate schemes, which facilitates huge computation time savings in modal-based optimization with static aeroelastic considerations. The accuracy of the modal approach has been shown to be very high in several realistic static-aeroelastic design studies[5,7,10-12].

Stress/Strain Analysis

Element stresses and strains can be related to the structural displacements by

$$\{\sigma\} = [\mathrm{SU}_l]\{u_l\} \quad (7)$$

where $[\mathrm{SU}_l]$ is a fixed matrix and $\{u_l\}$ is a subset of $\{u_a\}$, obtained after clamping n_r selected degrees of freedom to eliminate rigid-body displacements. One can calculate the displacement vector by the basic modal assumption of Eq. (2), but the adequacy of the substitution of the resulting $\{u_l\}$ in Eq. (7) for calculating stresses is questionable. References 10-12 showed that, with a fair number of elastic modes (typically 20-50) taken into account, the basic modal assumption is adequate for stress analysis, but only when the baseline structure is considered. When applied to a modified structure, the use of baseline modes might yield grossly inaccurate stresses and strains. The most accurate way to perform stress/strain analysis is by updating the full finite-element stiffness matrix and solving for displacements under the updated loads of Eq. (6). This hybrid approach (modal-based trim followed by full-order stress analysis) is easy to implement when the modal and discrete schemes are integrated in one code[11]. It is much less inefficient, however, than the modal-based alternatives discussed below.

Reference 7 modified the basic modal approach by supplementing the modal data base with modal perturbations. The first-order displacement vector for stress and strain analyses of the modified structure is expressed as

$$\{u_l\} = \{u_l\}_b + \{\Delta u_l^{(1)}\} \quad (8)$$

where $\{u_l\}_b$ is the elastic displacement of the baseline structure under the modified net loads, and $\{\Delta u_l^{(1)}\}$ is the incremental displacement change due to forces applied by the added material on the baseline structure. The first term of Eq. (8) can be formulated by the mode-displacement (MD) approach as[9]

$$\{u_l\}_{b_{MD}} = [\phi_{le}]\times \left([I] + [K_{ee}]_b^{-1}\left[\sum_{i=1}^{n_{dv}}(v_i - v_{b_i})[K_{ee}]_i\right]\right)\{\xi_e\} \quad (9)$$

where $[K_{ee}]_b$ is the generalized stiffness matrix of the baseline structure and $[K_{ee}]_i$ is its derivative with respect to the ith design variable v_i. Alternatively, when the discrete and modal-based codes are integrated, it is more effective to use the summation-of-force (SOF) approach using the already decomposed baseline stiffness matrix $[K_{ll}]_b$ to calculate

$$\{u_l\}_{b_{SOF}} = [K_{ll}]_b^{-1}\{P_l\} \quad (10)$$

where $\{P_l\}$ is the $\{u_l\}$-related subset of $\{P_a\}$ of Eq. (6). Comparisons between the use of the MD and SOF approached in modal-based optimization are given in Refs. 11 and 12.

The second term in Eq. (8) is

$$\{\Delta u_l^{(1)}\} = [K_{ll}]_b^{-1}\left[\sum_{i=1}^{n_{dv}}(v_i - v_{b_i})[\phi_{Fl}]_i\right]\{\xi_e\} \quad (11)$$

where

$$[\phi_{Fl}]_i = -\frac{\partial[K_{ll}]}{\partial v_i}[\phi_{le}]$$

are modal force perturbation matrices that are stored in the data base before the optimization starts[10]. Analytical expressions for the sensitivity of stress and strain constraints in design maneuver load cases, which take into account loads redistribution effects, are given in Refs. 10 and11. Ref. 11 used the first-order displacement approximation of Eq. (8) to calculate higher order approximations in an iterative process. It improved the accuracy of the resulting stresses, but somewhat slowed down the modal-based process. In an optimization process based on several design steps, it is more effective to use the first-order displacement vector at one step for defining a generalized coordinate that expands the modal basis in the following step, as shown below.

Expanded Modal Matrices

Static modes can be added to the modal basis after the baseline analysis and the first design step are completed. The starting point in defining an additional mode is the incremental displacement change of Eq. (11), as calculated in the previous design iteration, which can be expressed as

$$\{\bar{\phi}_{ls}\} = [K_{ll}]_b^{-1}\{\bar{P}_l\} \quad (12)$$

where

$$\{\bar{P}_l\} = \left[\sum_{i=1}^{n_{dv}}(v_i - v_{b_i})[\phi_{Fl}]_i\right]\{\bar{\xi}_e\}$$

where $\{\bar{\xi}_e\}$ is the vector of generalized elastic deflections in the previous iteration.

The deflection vector $\{\bar{\phi}_{ls}\}$ is orthogonalized with respect to baseline modes $[\phi_{le}]$ by

$$\{\phi_{ls}\} = \{\bar{\phi}_{ls}\} - [\phi_{le}][\mathrm{GK}_{ee}]_b^{-1}[\phi_{le}]^T\{\bar{P}_l\} \quad (13)$$

which can be shown, by using Eqs. (A-7), (2-3) and (12), to be orthogonal to the existing modal coordinates with respect to the baseline stiffness matrix, namely

$$[\phi_{le}]^T[K_{ll}]_b\{\phi_{ls}\} = \{0\} \quad (14)$$

The first static mode is added in the second iteration, with Eq. (12) calculated with the original data-base matrices and the baseline $\{\bar{\xi}_e\}$ of n_e modes. The data-base matrices are then expanded such that the analysis and sensitivity of the modified structures can be performed as described in Ref. 11, but with the expanded basis of $n_z = n_e + 1$ modes. The baseline modes matrix is expanded by

$$[\phi_{lz}] = \begin{bmatrix} \phi_{le} & \phi_{ls} \end{bmatrix} \quad (15)$$

The baseline generalized stiffness matrix becomes

$$[K_{zz}]_b = \begin{bmatrix} K_{ee_b} & 0 \\ 0 & K_{ss} \end{bmatrix} \quad (16)$$

where, as implied by Eqs. (12)-(14), the added diagonal term is

$$K_{ss} = \{\phi_{ls}\}^T[K_{ll}]_b\{\phi_{ls}\} = \{\phi_{ls}\}^T\{\bar{P}_l\} \quad (17)$$

The baseline $[M_{er}]$ in Eq. (3) is expanded by

$$[M_{zr}]_b = \begin{bmatrix} 0 \\ \{\phi_{as}\}^T[M_{aa}]_b[\phi_{ar}] \end{bmatrix} \quad (18)$$

where $\{\phi_{as}\}$ is the merge of $\{\phi_{ls}\}$ and zeros at the n_r clamping coordinates discussed after Eq. (7).

Subsequent iterations are performed with the expanded data-base matrices. New static modes are calculated at the end of each iteration. These modes affect the model in one of three ways:

1. If the number of already added modes n_s is equal to a maximum number $n_{s_{max}}$ specified by the user, the new mode is orthogonalized with respect to the first $n_e + n_s - 1$ modes and then simply replaces the last added mode.
2. If $n_s < n_{s_{max}}$, the new mode is orthogonalized with respect to all the existing $n_e + n_s$ modes and its K_{ss_j} value is calculated. If $K_{ss_j} > K_{ee_1} \times 10^{-6}$ (of the first elastic mode), the mode is added to the generalized coordinates as described above (with the already added static modes treated as normal modes).
3. If $K_{ss_j} \leq K_{ee_1} \times 10^{-6}$, the new mode is not added to avoid singularity of the expanded $[K_{zz}]_b$.

The aerodynamic force coefficients associated with the added modes are used to expand the generalized aero matrices in the static aeroelastic trim and loads equations. In this way, the added modes improve also the accuracy of the aeroelastic trim and effectiveness solutions along the optimization path, which were not affected by the model perturbations of the previous section.

Numerical Example

The numerical example is based on a generic Advanced Fighter Composite-wing (AFC) ASTROS model with an all movable horizontal tail and four control surfaces on each wing where only the two trailing-edge ones used for maneuvering. The USSAERO[1] aerodynamic model is shown in Figure 1. The structural model consists of 1276 grid points and 4449 elements, and has 3762 free degrees of freedom with symmetric boundary conditions and 3797 with anti-symmetric ones. Top view of the of the entire aircraft and of the wing structural models is shown in Figures 2 and 3. The wing box is divided into 13 zones. The thickness of the 0, ±45 and 90 deg direction plies in the upper and lower skins are used as design variables (for a total of 78 design variables). The structural arrangement and the design zones are identical to those used in Refs. 10-12, except that the wing skip there was made of aluminum.

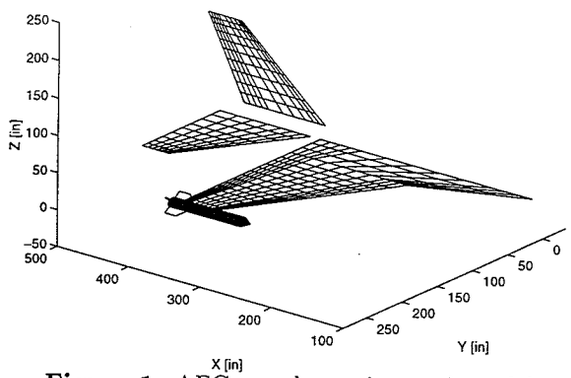

Figure 1: AFC aerodynamic panel model

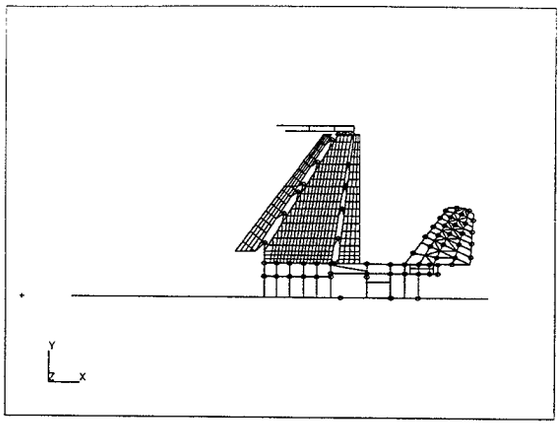

Figure 2: AFC wing-tail-fuselage structural model

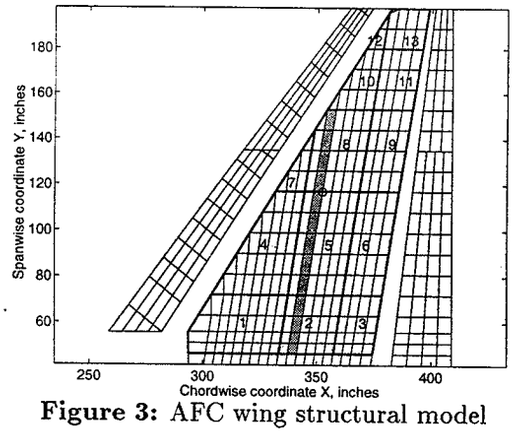

Figure 3: AFC wing structural model

The wing box was first optimized for minimum weight under the strain constraints of the 9g symmetric pull-up maneuver in Table 1. Modal-based optimization runs were performed with 48 symmetric elastic modes and 49 anti-symmetric ones. Results for modal runs with various strain analysis options, with and without static modes added to the modal basis, are compared below with results obtained by a standard discrete-coordinate ASTROS run. Optimization histories for the reference discrete optimization case, and for various modal-based options without adding static modes, are compared in Figure 3. It can be observed that even without expanding the modal basis the overall accuracy of the modal-based optimization is quite good, even though the weight of the changeable elements is reduced by a total of 30%. The effects of adding one and two static modes to the modal data base are shown in figures 5 and 6. The effect of adding one static mode is similar to that of the 2nd order approximation in Figure 4, except that the small difference between the discrete and hybrid curves in Figure 4 (which is not affected by high-order approximations) has disappeared. With two static modes added (Figure 6), all methods give practically the same results.

Load Condition	Design Constraint
Mach 0.95, 10,000 ft, 9g pull-up	fiber strain: $3000\mu\epsilon$ tension, $2800\mu\epsilon$ compression
Mach 1.20, Sea Level, -3g push-over	fiber strain: $3000\mu\epsilon$ tension, $2800\mu\epsilon$ compression
Mach 0.95, 10,000 ft, max steady roll	aileron effectiveness ≥ 0.2373
Mach 1.20, Sea Level, max steady roll	roll rate constraint

Table 1: Design loads and constraints

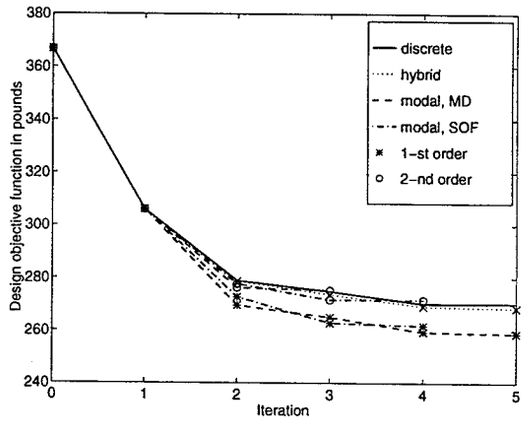

Figure 4: One-case optimization weight history without static modes

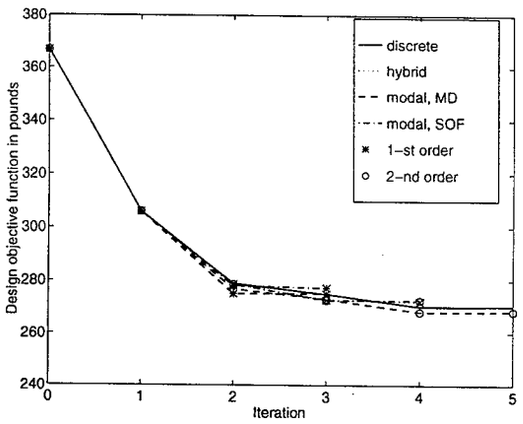

Figure 5: One-case optimization weight history with one static modes

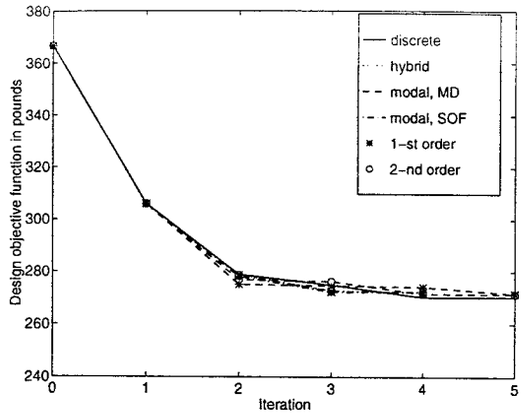

Figure 6: One-case optimization weight history with two static modes

The accuracy of the various modal options is investigated with the design variables that were obtained after the 1st-order MD optimization case with one static mode. The total weight of the designed elements is at this stage (275.1 *lb*) is 25 % lower than that of the baseline structure (366.7 *lb*). The various modal options were used to calculate the trim parameters and the principal strains along the wing span using the data base of the baseline structure. The regular discrete-coordinate approach was also applied to the model to comparison.

The trim parameters for the discrete, modal, and modal with static mode (MSM) methods are given in Table 4.1. MSM results are no given for the baseline case because the static mode is added only after the 1st design step. The modal trim results are very close to the discrete ones even without adding the static mode, and the effect of the added mode on the trim variables is negligible. This shows that the effects of expanding the modal basis shown below are due to the effects on local strains.

Structure	Trim param.	Method		
		Discrete	Modal	MSM
Baseline	α [deg]	8.191	8.214	–
	δ [deg]	-4.222	-4.253	–
Modified	α [deg]	8.129	8.155	8.152
	δ [deg]	-4.301	-4.321	-4.327

Table 4.1: Trim parameters at 2-nd design step in 1-case optimization

The errors of the principal stains (compared to the discrete-coordinate case)

in terms of percentage of the maximum allowable strain in tension, along the skin elements marked in Figure 3, are shown in figure 7 for various modal options. It can be observed that the effect of adding the static mode is most significant in the SOF case (all errors become smaller than 0.3%), and that the hybrid stresses are almost perfect even without adding the mode.

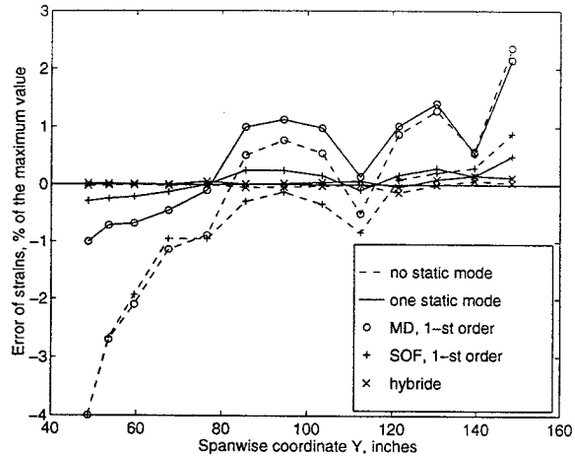

Figure 7: Errors of the principal strains along the wing span

The wing box was next optimized for minimum weight under the simultaneous strain, aileron effectiveness and roll-rate constraints specified in Table 1. Optimization histories for the reference discrete optimization case, and for various modal-based options without adding static modes, are compared in Figure 8. The total weight errors with the 1st-order approximation where 2-4% while those of the hybrid and 2nd-order methods were 0-1%. The same optimization cases, but with a single static mode added to the modal basis are shown in Figure 9. Now all the fully modal cases are within 1% of the discrete case, and the hybrid case converges to the discrete one exactly in spite of the slight error after the first design step.

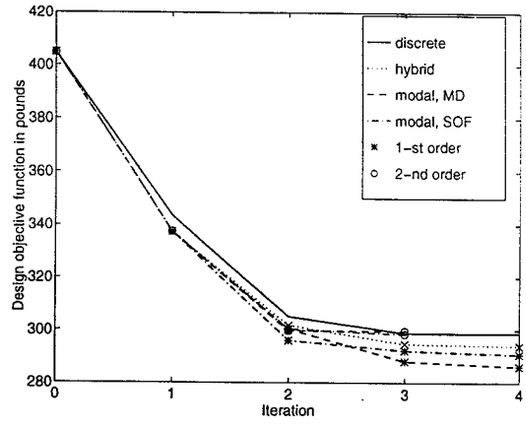

Figure 8: Four-case optimization weight history without static modes.

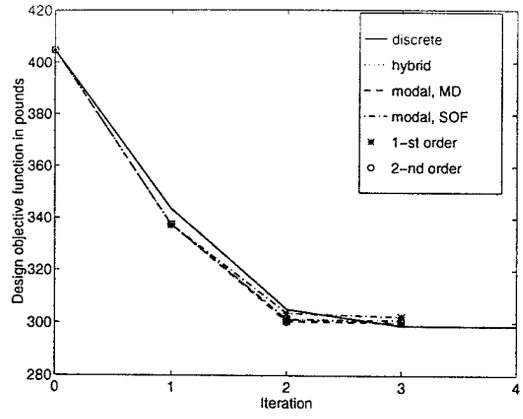

Figure 9: Four-case optimization weight history with one static mode.

The skin principal-strain RMS errors of the various modal techniques, calculated at the 2nd iteration of Figure 9, relative to the discrete strains, are shown in Figure 10 in percentage of the maximum allowable strain in tension. The CPU time per design iteration in the various options, not including the set-up time for constructing the data base, are given in Table 2. The set-up CPU time for constructing the data base was 578 seconds. The CPU time for running the discrete case was 311 seconds in the preface stage and then 501 seconds per iteration. The SOF modal case with one static mode is probably the most cost effective option in our case. It reduces the CPU time per iteration by 82% compared to the discrete case, with RMS skin strain errors of 0.2%. The set-up time for constructing the modal data base is not very important because the same data base can be used for numerous optimization cases with various move limits, constraints and control gearing ratios.

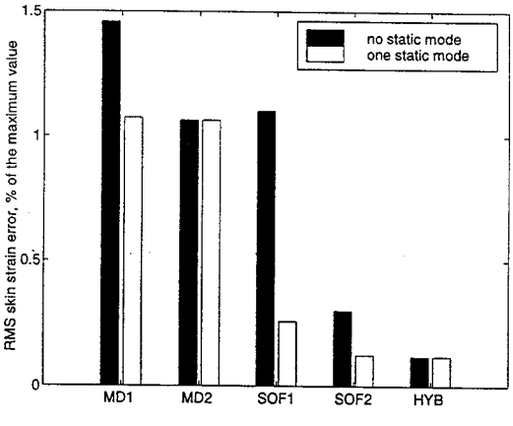

Figure 10: RMS skin principal strains errors.

Method	Static mode	
	no	one
Hybrid		
1st design iter.	34.0	34.0
other iter.	107.0	153.0
SOF		
1st design iter.	38.5	38.5
other, 1st order	62.7	90.9
other, 2nd order	176.6	204.8
MD		
1st design iter.	31.5	31.5
other, 1st order	56.9	86.0
other, 2nd order	175.7	203.9

Table 2: CPU seconds for design iterations with modal methods.

Conclusions

The modal-based structural optimization method was extended to allow the expansion of the modal data base with static modes calculated during the design process. The expanded basis improves the accuracy of the modal approach and yields asymptotic convergence to the exact discrete-coordinate design. It also allows larger weight changes (more than 30% reduction in the analyzed cases) with a relatively small computational cost. The improvements module as an on-line multi-disciplinary design tool. The composite-wing case studies were with relatively large number of design variables. They were indicative that the modal approach for aeroelastic design has great potential for the early preliminary design of aircraft where answers to "what if" type questions are needed in short order. The modal approach is accurate to produce quite similar results to the discrete approach.

Acknowledgments

This work was partially supported by the Israeli Ministry of Immigrant Absorption, and partially by a contract with Lockheed Martin Tactical Aircraft Systems.

References

1. Neill, D.J., Johnson, E.H., and Confield, R., "ASTROS - A Multidisciplinary Automated Structural Design Tool", Journal of Aircraft, Vol. 27, No. 12, 1990, pp. 1021-1027.
2. Climent, H., Johnson, E.H., "Aeroelastic Optimization Using MSC/NASTRAN", Proceedings of the International Forum on Aeroelasticity and Structural Dynamics, Strasbourg, France, May 1993, pp 1097-1116.
3. Livne, E., Schmit, L. A. and Friedmann, P. P., "Integrated Structure/Control/Aerodynamic Synthesis of Actively Controlled Composite

Wings", Journal of Aircraft, Vol. 30, No. 3, 1993, pp. 387-394.

4. Bindolino, G., Lanz, M., Mantegazza, P. , and Ricci, S., "Integrated Structural Optimization in the Preliminary Aircraft Design", Proceedings of the 17th Congress of the International Council of the Aeronautical Sciences, Stockholm, Sweden, September 1990, pp. 1366-1378.
5. Karpel, M. and Sheena, Z., "Structural Optimization for Aeroelastic Control Effectiveness", Journal of Aircraft, Vol. 26, No. 8, 1989, pp. 493-495.
6. Karpel, M., "Multidisciplinary Optimization of Aeroservoelastic Systems Using Reduced-Size Models", Journal of Aircraft, Vol. 29, No. 5, pp. 939-946.
7. Karpel, M. and Brainin, L., "Stress Considerations in Reduced-Size Aeroelastic Optimization", AIAA Journal, Vol. 33, No. 4, 1995, pp. 726-722.
8. Karpel, M., and Presente, E., "Structural Dynamic Loads in Response to Impulsive Excitation", Journal of Aircraft, Vol. 32, No. 4, 1995, pp. 853-861.
9. Karpel, M. and Raveh, "Fictitious Mass Element in Structural Dynamics", AIAA Journal, Vol. 34, No. 3,1996, pp. 607-613.
10. Karpel, M., Moulin, B. and Love, M.H., "Modal-Based Structural Optimization with Static Aeroelastic and Stress Constraints", Journal of Aircraft, Vol. 34, No. 3, 1997, pp. 433-440.
11. Karpel, M., "Modal Based Enhancement of Integrated Structural Design Optimization Schemes", Proceedings of the AIAA/NASA /ISSMO 6th Symposium on Multidisciplinary Analysis and Optimization, Bellevue, Washington, September 1996, pp. 1223-1232.
12. Moulin, B. and Karpel, M., "Static Condensation in Modal-Based Structural Optimization", Proceedings of the 37th Israel Annual Conference on Aerospace Sciences, Israel, February 1997, pp. 332-341.
13. Kirsch, U., "Reduced Basis approximations of Structural Displacements for Optimal Design", AIAA J. Vol. 29, 1991, pp. 1751-1758.
14. Kirsch, U., "Improved Stiffness-Based First-Order Approximations for Structural Optimization", AIAA J., Vol. 33, 1995, pp. 143-150.

Appendix A:
Discrete Coordinates and Matrices

Common finite-element codes such as NASTRAN start the construction of the structural matrices at the individual element level. The contribution of each element is transformed to the global (g-set) coordinate system, which contains 6 coordinates for each grid point, and added to the g-set stiffness and mass matrices, $[K_{gg}]$ and $[M_{gg}]$. At this preface stage, the matrices are not affected by modeling constraints, boundary conditions or solution method.

To avoid repetitive construction of the g-set matrices from scratch, The ASTROS optimization code separates the contributions of the structural parts which are affected by the n_{dv} global design variables from those which are not affected. A global design variable is a changeable factor that affects the structural matrices of a user-defined group of finite elements. In each design cycle, the matrices are assembled by adding the contributions of the changeable elements to the contribution of the unchangeable elements. The stiffness and mass matrices is assembled by

$$[K_{gg}] = [K_{gg}]_U + \sum_{i=1}^{n_{dv}} v_i \frac{\partial [K_{gg}]_L}{\partial v_i} + [K_{gg}]_{NL} \quad (A-1)$$

and

$$[M_{gg}] = [M_{gg}]_U + \sum_{i=1}^{n_{dv}} v_i \frac{\partial [M_{gg}]_L}{\partial v_i} + [M_{gg}]_{NL} \quad (A-2)$$

where v_i is the current value of the ith design variable, subscript U denotes the unchangeable portion of the matrices, L denotes the assembly of element matrices which are linearly depended on v_i, and NL denotes the assembly of those which are non-linear functions of v_i. The contributions of most finite elements in typical aerospace models are linear with respect to a representative gage. Hence, optimization of aircraft structures can be usually formulated with the non-linear terms omitted.

The g-set matrices are reduced to the free (f-set) coordinates by application of single- and multi-point constraints (SPC and MPC). This reduction to $[K_{ff}]$ and $[M_{ff}]$ is repeated in each discrete-coordinate design iteration. ASTROS defines these constraints as "boundary conditions" and allows simultaneous optimization runs with different sets of boundary conditions.

NASTRAN and ASTROS allow a further reduction of the structural matrices by Guyan's static condensation. The f-set coordinates are divided into analysis (a-set) and omitted (o-set) ones, and the undamped equation of motion is partitioned accordingly,

$$\begin{bmatrix} \bar{K}_{aa} & K_{ao} \\ K_{ao}^T & K_{oo} \end{bmatrix} \begin{Bmatrix} u_a \\ u_o \end{Bmatrix} + \begin{bmatrix} \bar{M}_{aa} & M_{ao} \\ M_{ao}^T & M_{oo} \end{bmatrix} \begin{Bmatrix} \ddot{u}_a \\ \ddot{u}_o \end{Bmatrix}$$

$$= \begin{Bmatrix} \bar{P}_a \\ P_o \end{Bmatrix} \quad (A-3)$$

It is assumed that the inertia loads can be neglected in the bottom row, which yields

$$\{u_o\} = [G_o]\{u_a\} + [K_{oo}]^{-1}\{P_o\} \qquad (A-4)$$

where

$$[G_o] = -[K_{oo}]^{-1}[K_{ao}]^T \qquad (A-5)$$

It is also assumed that the o-set accelerations can be approximated by

$$\{\ddot{u}_o\} = [G_o]\{\ddot{u}_a\} \qquad (A-6)$$

The resulting a-set equation of motion is

$$[K_{aa}]\{u_a\} + [M_{aa}]\{\ddot{u}_a\} = \{P_a\} \qquad (A-7)$$

where

$$\begin{aligned} [K_{aa}] &= [\bar{K}_{aa}] - [K_{ao}][K_{oo}]^{-1}[K_{ao}]^T \\ [M_{aa}] &= [\bar{M}_{aa}] + [M_{ao}][G_o] + [G_o]^T[M_{ao}]^T \\ &+ [G_o]^T[M_{oo}][G_o] \\ \{P_a\} &= \{\bar{P}_a\} + [G_o]^T\{P_o\} \end{aligned}$$

Equation (A-7) can be used for normal modes analysis (with $\{P_a\} = 0$), for dynamic response (with an additional damping term), or for static analysis with inertial-relief effects (with $\{\ddot{u}_a\}$ defined by rigid-body accelerations).

A further reduction is required when the structure has n_r rigid-body degrees of freedom. User-selected n_r a-set coordinates are used to represent the rigid-body (r-set) motion, while the left-over (l-set) coordinates define the relative elastic deformations. While $[K_{aa}]$ is a singular matrix when $n_r > 0$, $[K_{ll}]$ is not and hence can be inverted.

The transformation matrices between the coordinate sets are saved in the data base at the initial analysis phase for subsequent recovery of the displacements from the lowest l-set level to the highest g-set level, and for reduction of g-set loading vectors to lower sets. The modal approach, which does not update the discrete-coordinate stiffness and mass matrices in each design step, uses a recovery/reduction process to calculate stiffness or mass dependent loading vectors. To calculate the inertia loads $\{P_a\} = [M_{aa}]\{\ddot{u}_a\}$, for example, $\{\ddot{u}_a\}$ is first expanded to the g-set $\{\ddot{u}_g\}$, multiplied by the components of $[M_{gg}]$ given above, summed according to the current values of the design variables, and then reduced to the a-set level.